Brain Stimulation 17 (2024) 1265–1276

Contents lists available at ScienceDirect

Brain Stimulation

journal homepage: www.journals.elsevier.com/brain-stimulation

The role of white matter variability in TMS neuromodulatory effects

Mar Martín-Signes [a,b,*,1], Pablo Rodríguez-San Esteban [a,b,1], Cristina Narganes-Pineda [a,b], Alfonso Caracuel [a,c], José Luís Mata [a,d], Elisa Martín-Arévalo [a,b], Ana B. Chica [a,b]

[a] Mind, Brain and Behavior Research Center (CIMCYC), University of Granada, Spain
[b] Department of Experimental Psychology, Faculty of Psychology, University of Granada, Spain
[c] Department of Developmental and Educational Psychology, Faculty of Psychology, University of Granada, Spain
[d] Department of Personality, Evaluation and Psychological Treatment, Faculty of Psychology, University of Granada, Spain

ARTICLE INFO

Keywords:
Alerting
Attention
Diffusion weighted imaging
DWI
Spatial
TMS
White matter

STRUCTURED ABSTRACT

Background: Transcranial Magnetic Stimulation (TMS) is a widely used tool to explore the causal role of focal brain regions in cognitive processing. TMS effects over attentional processes are consistent and replicable, while at the same time subjected to individual variability. This individual variability needs to be understood to better comprehend TMS effects, and most importantly, its clinical applications.
Objective: This study aimed to explore the role of white matter variability in TMS neuromodulatory effects on behavior in healthy participants (N = 50).
Methods: Participants completed an attentional task in which orienting and alerting cues preceded near-threshold targets. Continuous Theta Burst Stimulation (cTBS) was applied over the left frontal eye field (FEF) or an active vertex condition. White matter was explored with diffusion-weighted imaging tractography and Tract-Based Spatial Statistics (TBSS).
Results: Behaviorally, TMS over the left FEF slowed down reaction times (especially in the alerting task), impaired accuracy in the objective task, and reduced the proportion of seen targets (as compared to the vertex condition). Attentional effects increased, overall, when TMS was applied to the left FEF as compared to the vertex condition. Correlations between white matter and TMS effects showed i) reduced TMS effects associated with the microstructural properties of long-range white matter pathways such as the superior longitudinal fasciculus (SLF), and interhemispheric fibers of the corpus callosum (CC), and ii) increased TMS effects in participants with high integrity of the CC connecting the stimulated region with the opposite hemisphere. Additionally, variability in attentional effects was also related to white matter, showing iii) increased alerting effects in participants with low integrity of association, commissural, and projection fibers, and iv) increased orienting effects in participants with high integrity of the right SLF III.
Conclusion: All these observations highlight the importance of taking into account individual variability in white matter for the understanding of cognitive processing and brain neuromodulation effects.

1. Introduction

Behavioral effects of Transcranial Magnetic Stimulation (TMS) can exhibit significant inter-individual differences [1,2]. Part of this variability may be attributed to individual differences in functional or structural connections in the brain networks directly or indirectly associated with the stimulated area [3,4]. Stimulating a brain area not only changes its functioning but also affects structurally or functionally connected regions [3–6]. Thus, considering these individual differences is crucial when interpreting TMS neuromodulation effects in a causal manner [7].

Some studies have explored changes in functional connectivity when specific brain areas are stimulated [4,5], reporting that individual baseline differences in functional connectivity impact behavioral TMS effects [1]. Other studies suggest that TMS pulses propagate through white matter fasciculi [3,6,8,9] and the integrity of these fasciculi shapes the spread of action potentials [10]. It has also been proposed that structural links can predict network-level responses to perturbation

* Corresponding author. Department of Experimental Psychology, Faculty of Psychology, Campus of Cartuja, University of Granada, 18011, Granada, Spain.
E-mail address: msignes@ugr.es (M. Martín-Signes).
[1] Shared first authorship.

https://doi.org/10.1016/j.brs.2024.11.006
Received 8 July 2024; Received in revised form 23 October 2024; Accepted 8 November 2024
Available online 10 November 2024

more accurately than functional connectivity [11]. This may be explained by the fact that the functional connectivity of certain brain networks depends, in part, on their anatomical connectivity [12].

In psychophysical experiments in which we have manipulated attention and measured its influence on perception, we have studied whether individual differences in white matter microstructure influence TMS neuromodulation effects over behavior. We have found reduced TMS effects in participants with increased integrity in tracts like the superior longitudinal fasciculus (SLF), which connects the parietal and frontal cortex [13–15]. That is, participants with greater integrity in tracts associated with key attentional regions showed less interference in the face of external perturbations by TMS than participants with lower integrity in these tracts. In these studies, the correlated fasciculus did not directly innervate the targeted area. These results have been interpreted as indicative of a compensatory effect. As suggested elsewhere [16], after the disruption of a brain region, there is a flexible redistribution in cognitive networks, wherein other brain regions within the network or alternative cognitive networks may have the potential to partially compensate for the impaired function (e.g., Ref. [17]). We hypothesize that the effectiveness of the structural connection (reflected in microstructural properties of white matter) between regions of relevant alternative networks may contribute to more efficient compensatory processes.

Relatively recent studies have also shown the importance of the corpus callosum (CC) in the rehabilitation of attentional functions after brain damage [18–21]. The integrity of these interhemispheric fibers seems crucial for compensatory processes following brain damage, and perhaps for more transient perturbations such as those produced by TMS. For example, using a visual search task, Chechlacz et al. [22] showed that microstructural properties of the CC correlated with TMS effects: the higher the integrity of the CC, the stronger the leftward shifts in attention after stimulation over the left intraparietal sulcus (IPS). These results were explained by a model proposing a role of the CC in both information transfer between hemispheres [23] and interhemispheric inhibition ([24], see also [25]).

Our studies exploring the role of white matter variability in TMS neuromodulation effects have focused on the attentional system and the causal role of key regions of the attentional networks [26] and the white matter fasciculi connecting these regions [27]. In the present study, we focused on two attentional networks, the alerting and the orienting networks, whose functioning is mediated by dorsal regions including the frontal eye field (FEF) and the IPS. However, while the activation of this network is bilateral during orienting [26], activations during alerting tasks are more left-lateralized [28–30]. In particular, the left FEF showed significant activations in two previous functional Magnetic Resonance Imaging (fMRI) studies where we manipulated alerting [31] and orienting [32] while participants responded to near-threshold visual targets.

This study aimed to investigate i) the causal influence of the left FEF on orienting and alerting attentional systems, and ii) the impact of white matter variability on TMS neuromodulatory effects on behavior in the healthy brain. Additionally, we explored whether white matter variability could explain behavioral attentional effects in the absence of stimulation (i.e., in the control vertex condition). It is well known that attentional capacities largely vary between individuals [33] and part of this variability might be explained by white matter structural properties [22,25,27,34–36].

To achieve these aims, this study used a substantial sample of participants (N = 50) to ensure high statistical power and promote replicability. Previous results were based on studies with samples of around 20 participants, which were designed with different objectives than exploring the role of white matter in the variability of TMS effects [13–15,37]. This study aims to confirm the results of previous research, which is essential for the advancement of a robust and transparent science. We used a perceptual task in which spatial attention and phasic alerting were manipulated before target presentation. Continuous Theta Burst Stimulation (cTBS) – a well-established inhibitory protocol – was used to interfere with the functioning of an attentional region (i.e., the left FEF), while exploring whether white matter microstructural properties correlated with behavioral TMS modulations or attentional effects (i.e., for the control vertex condition). To perform these white matter and function correlations, individual diffusion-weighted imaging (DWI) tractography of the SLF and the CC was performed. The selection of these white matter tracts was based on the previous literature, reviewed above. However, this approach may overlook the involvement of other tracts or white matter areas that could also impact the effects of TMS. The present research introduced a whole-brain data-driven analysis approach to ensure that potentially relevant associations between TMS/attentional effects and white matter integrity were not missed. We used Tract-Based Spatial Statistics (TBSS), a method comprising voxel-wise statistical analysis that allows such investigation across the entire brain. This approach will contribute to identifying unexplored targets, paving the way for future research.

Behaviorally, if the left FEF is causally relevant for attentional orienting, inhibitory TMS over this region should reduce the attentional effect (as compared to the vertex condition). Given the known role of the FEF in both attention and perception [38–40], inhibitory TMS over this region could also impair overall response times and target detection. We hypothesized that these effects would correlate with the integrity of the SLF, such that greater integrity of this fasciculus would result in reduced TMS effects [13–15]. Based on studies of patients with brain damage [19–21] and healthy participants [22], we also hypothesized that greater fiber integrity of the CC would lead to greater TMS effects. We expected alerting effects to be related with the integrity of tracts of the anterior alerting system [25,34], and left fronto-parietal tracts [36], although we did not have specific hypotheses about the direction of the effect [35,36]. Given the extensive evidence of the role of the SLF in spatial orienting (from neglect patients [41–44], and healthy population, [27,45]), we expected a positive association between SLF integrity and orienting effects. This study aims to advance our understanding of individual differences observed in neuromodulation processes in particular, and attentional functioning in general, which might be crucial for improving research and clinical practice.

2. Methods

2.1. Participants

G*Power [46] was used to calculate a priori sample size for the multiple regressions conducted, in which TMS effects were predicted using the anisotropy of the SLF (6 branches; [27,47]) and the CC (7 portions; [48]). Previous research has reported medium effect size for correlations (effect size was 0.4 for [21], and 0.6 for [15]), therefore, we calculated the effect size for a medium $r^2 = 0.3$, $f^2 = 0.428$, $\alpha = 0.05$, power = 0.8, number of predictors = 7. Based on this calculation, a sample of 42 participants was estimated. The final study sample included 50 volunteers (39 females, mean age 21.57 years, SD = 4.54). All participants were right-handed and had normal or corrected-to-normal vision, and no prior experience with the task. No participant had a history of major medical, neurological, or psychiatric disorders, and followed all the safety requirements to undergo MRI and TMS studies [49]. Participants received a monetary compensation of 10€/h for their participation. Signed informed consent was collected prior to their inclusion in the study. Participants were informed about their right to withdraw from the experiment at any time. The University of Granada's Research Ethics Committee approved the experiment (#554/CEIH/2018), which was carried out in accordance with the Code of Ethics of the World Medical Association (Declaration of Helsinki) for experiments involving humans (last update: Brazil, 2013).

2.2. Apparatus and stimuli

E-Prime software version 2.0 [50] was used for stimuli presentation and behavioral data collection. Participants were seated at an approximate distance of 70 cm from the computer screen (LG Flatron L1718S-SN,17″, 1280 x 1024, 75Hz refresh rate). Trials started with a display composed of three boxes (4.8° × 5.3°), one in the center of the screen, and one at each side of it, presented against a grey background (RGB: 128, 128, 128). The fixation point consisted of a black cross (0.3° × 0.3°) that appeared in the center of the display. In the orienting blocks, a spatial cue (a black circle, 1° diameter), was presented at the outer edge of either the left or right box (see Fig. 1C). In the alerting blocks, an alerting tone (500 Hz frequency, 72 dB) was presented on 50 % of the trials. The target was a Gabor stimulus that could be presented in either one of the two peripheral boxes or could be absent. MATLAB 8.1 (http://www.mathworks.com) was used to generate 200 Gabor stimuli (spatial frequency 4 cycles/deg., 1.3° diameter, 0.1° SD) with a maximum and minimum Michelson contrast of 0.92 and 0.02, respectively. After the target presentation, two sets of arrows (>>> or <<<, 0.2° × 0.9°) were displayed above and below the fixation point, at a distance of 0.9°, pointing to the lateral boxes.

2.3. Task and procedure

The study consisted of three sessions, one in which participants underwent an MRI scan (see MRI data acquisition) and two TMS sessions (see TMS procedure; see also [14], for a similar protocol). The procedure of the two TMS sessions (Fig. 1A) was similar in all aspects except for the stimulated region (left FEF or vertex) and the individual resting motor threshold (rMT) measurement, that was only carried out in the first TMS session.

The TMS sessions started with a titration block, to adjust the percentage of seen targets individually. Titration trials were identical to the experimental trials, with the exception that they did not involve the use of alerting or orienting cues. All participants started with a suprathreshold Gabor to get familiarized with the procedure and the response keys. After this initial block, Gabor contrast was adjusted depending on participants' performance. After every 15 trials, if the percentage of seen stimuli was greater than 60 %, contrast was decreased in 0.5 points (in a scale of 200 different contrasts levels). If, on the contrary, the percentage of seen stimuli was lower than 40 %, contrast was increased in 0.5 points. When the percentage of seen targets ranged between 60 % and 40 % in two consecutive blocks, the titration procedure concluded, and this contrast was used for the rest of the experimental blocks in the session. After the titration procedure, the TMS protocol was delivered in one of the brain regions (see TMS procedure). After the stimulation, the participant started the experimental blocks of the task.

The sequence of events in each trial is shown in Fig. 1C. All trials started with the fixation display (500, 1000 or 1500 ms). Then the cue was presented (16 ms), consisting of a visual signal in the orienting blocks and an auditory signal in the alerting blocks, followed by an inter-stimulus-interval (ISI, 218 ms). After the ISI, the target was displayed (32 ms). It could be present (62 % of the trials) in either the left or the right box, or it could be absent (38 % of the trials). Participants had to give two consecutive responses. First, they were asked to report the orientation of the lines composing the Gabor stimulus (objective response), using their right hand to press the right or left mouse buttons, depending on the orientation of the lines. They were encouraged to respond as quickly and accurately as possible, with a time limit of 1968 ms. This task is referred to as objective because it was designed as a forced-choice task where there was a correct response. If they did not perceive the stimulus, they were instructed to respond randomly. Subsequently, participants were asked to report if they consciously perceived the target (subjective response). They made their response by selecting one of two arrows (>>> or <<<) pointing to the two possible target locations (right or left box). The arrows were presented randomly in each trial, above and below the fixation cross. Participants indicated the target's location by pressing the 'D' key corresponding to the upper arrow or the 'C' key corresponding to the lower arrow. They could also press the spacebar if they did not perceive the target. This response screen was displayed for 3000 ms. Participants were instructed to respond as accurately as possible and only when they were confident about their perception.

The task was composed of eight blocks, four belonging to the

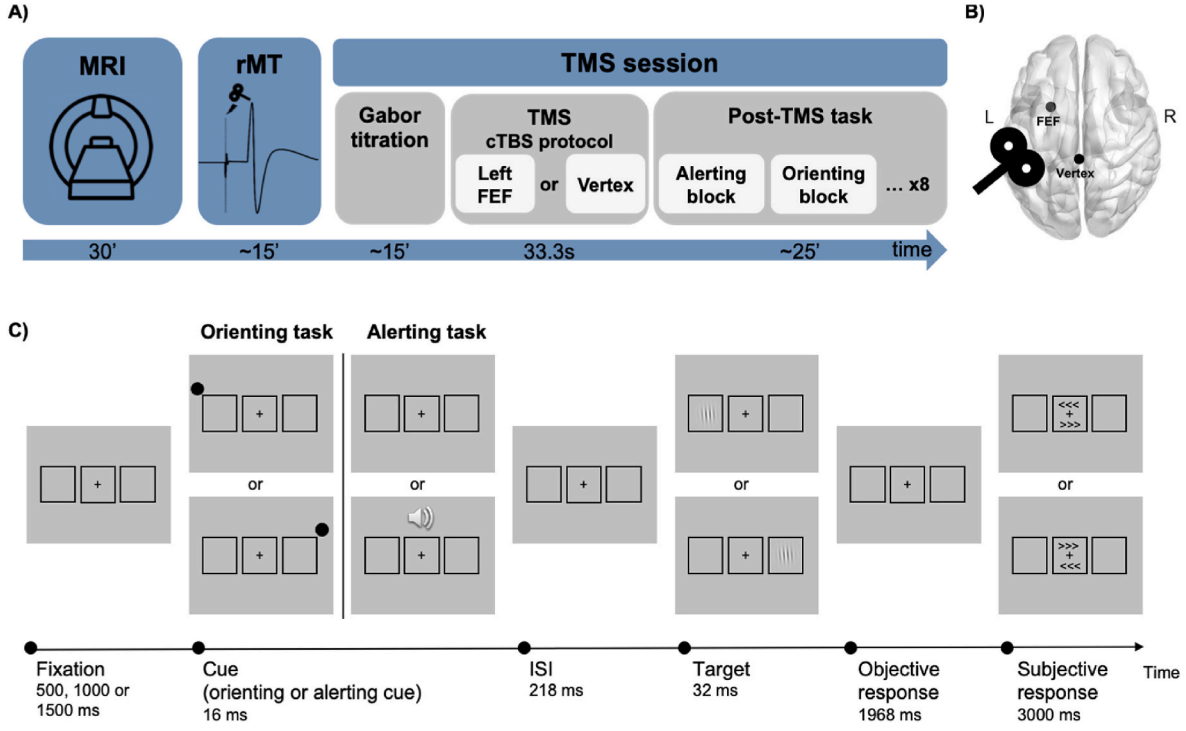

Fig. 1. (A) Schematic representation of the experimental procedure. (B) TMS regions. (C) Schematic representation of a trial in the orienting and alerting tasks.

orienting condition (59 trials per block; 236 trials in total) and four to the alerting condition (39 trials per block; 156 trials in total). The total duration of the task after stimulation was approximately 25 min. Half of the participants started with the orienting condition while the other half started with the alerting condition, and the following blocks continued in an alternating order. Within each block, the trial type appeared randomly. In the orienting blocks, the peripheral cue was displayed in the same location as the Gabor stimulus in 75 % of the trials (valid trials) and in the opposite location in the remaining 25 % of the trials (invalid trials). On the other hand, during the alerting blocks, a tone occurred in half of the trials (tone present trials), while in the other half, the target was not preceded by any tone (tone absent trials). For statistical analysis, we referred to valid orienting trials and tone-present trials as attended, and to invalid orienting trials and tone-absent trials as unattended.

Eye movements were not controlled in this experiment due to the technical complexity of the set-up and the availability of resources. However, we ran a pilot experiment (N = 13) using an Eyelink 1000 (SR Research) eye-tracking system, and we established that participants broke fixation in only 3.87 % of the trials (SD = 1.93 %; 3.9 % for the orienting task, and 3.85 % for the alerting task). In this pilot sample, where eye movements were controlled, we observed the expected behavioral effects (data can be found at https://osf.io/4jg3f/).

2.4. TMS procedure

TMS was delivered by means of a biphasic repetitive stimulator (Super Rapid 2, Magstim, Whitland UK) and a 70-mm figure-of-eight coil (Magstim, Whitland UK) which was held tangentially to the skull with the axis of the coil angled 45° from the mid-sagittal axis (lateral to medial and caudal to rostral). A TMS neuronavigation system (Brainsight; Rogue Systems, Montreal, Canada) was employed, with the capacity to estimate and track in real time the relative position, orientation, and tilting of the coil on the sectional and 3D reconstruction of the participants T1 with a precision of 5 mm [51]. Brain regions were stimulated using a continuous theta burst stimulation (cTBS) protocol [52,53]. This protocol consisted of three 30 Hz pulses delivered every 200 ms, for a total of 600 pulses, for a duration of 33.3s. These pulses were applied at 80 % of the rMT, defined as the minimum stimulus intensity that elicits MEPs >50 mV in five out of ten consecutive trials [53,54]. The rMT (mean 66.7 % of maximal stimulator output, MSO) was determined for each participant in the first session of the experiment (see Ref. [37], for a detailed explanation of the procedure). The mean TMS intensity applied was 51.5 % of MSO (SD = 4.4). For each participant, the same TMS intensity was used for the left FEF and the vertex stimulation. The order of the left FEF and Vertex sessions was counterbalanced between participants. Scalp coordinates for the stimulation sites were located by using the native space of each participant's T1. The TMS stimulation site was the left FEF (Montreal Neurological Institute [MNI] coordinates: x = −29, y = −4, z = 55), which was selected by calculating the mean coordinates of the maximal response observed in the FEF from two previous fMRI studies in the lab (alerting task, [31]; orienting task, [32]) (see Fig. 1B). The control stimulation site was the vertex (MNI coordinates: x = 0, y = −34, z = 78; [37]), which was not expected to induce any specific behavioral effects [55]. For a representation of the induced electric field for each stimulation site over a standard brain see Supplementary Fig. 1.

2.5. MRI data acquisition

Structural images were collected on a 3-T Siemens Prisma MRI scanner at the Mind, Brain, and Behavior Research Center (CIMCYC) of the University of Granada, using a 64-channels whole-head coil. High-resolution T1-weighted anatomical images (Repetition Time [TR] = 2530 ms, Echo Time [TE] = 3.5 ms, flip angle = 7°, slice thickness = 1 mm, field of view [FOV] = 256 mm) were collected. A DWI multiband and multi-shell sequence was also collected (TR = 3500 ms, TE = 75 ms, voxel size = 1.8 mm^3 isotropic, FOV = 208 mm, multi-band acceleration factor = 3). We acquired, in consecutive sequences, 8 vol at b = 300 s/mm^2 (2 vol b-value = 0), 32 vol at b = 1000 s/mm^2 (6 vol b-value = 0), and 60 vol at b = 2000s/mm^2 (6 vol b-value = 0). For each volume, 81 near axial slices were collected with a posterior-anterior phase of acquisition. Additionally, the b-value 300 sequence was acquired with an anterior-posterior phase of acquisition to correct for phase-encoding direction-induced distortions [56].

2.6. Diffusion weighted imaging (DWI) analysis

DWI data pre-processing included eddy current-induced distortions and participant's movements correction using the *eddy* tool from the FMRIB Software Library [57]. Slices identified as outliers were interpolated with predictions generated by the Gaussian Process (which never exceeded 5 % of the total slices). Additionally, distortions induced by phase encoding were corrected using the *topup* toolbox from FSL [56]. Image quality control included a visual inspection of raw data and outputs of every processing step. Image quality was rated using a 4-point scale, with 1 = excellent, 2 = minor, 3 = moderate, and 4 = severe. All images were scored as 1 or 2. Additionally, an automated quality control was performed with the FSL's tool QUAD [58]. We reviewed the most relevant quality metrics reported by the tool (i.e., average relative and absolute motion, Signal-to-noise ratio (SNR), and eddy currents). The following threshold values were used for each quality metric: average relative and absolute motion <1 mm, SNR >20 s/mm^2, eddy current standard deviation < 0.1 [58]. No participant was excluded after visual and automated image quality control.

2.6.1. DWI tractography

Multishell spherical deconvolution [59] was performed with the algorithm parameters $\alpha = 2$, algorithm iteration = 400, and $\eta = 0.001$ and $\nu = 8$ as regularization terms, using the software StarTrack. Whole-brain deterministic tractography was performed using a modified Euler tractography algorithm (angle threshold = 45° and HMOA threshold = 0.0036). Dissections of the tracts of interest were performed with the software TrackVis [60] using a multiple-ROI approach.

For the delineation of the 3 branches of the SLF (SLF I, II, and III on the left and the right hemisphere; see Fig. 2A), three frontal ROIs around the white matter of the superior, middle, and inferior frontal gyri, and a ROI around the white matter of the parietal lobe were delineated (see Ref. [27,47], for a detailed explanation of the method). Streamlines of the arcuate fasciculus projecting to the temporal lobe were excluded by drawing an excluding ROI in the temporal white matter. Cingulate fibers were distinguished from the SLF I by delineating the frontal ROI above the cingulate sulcus.

The CC was delineated by using Witelson's proposed schema [48], which divides the CC into seven portions: 1) Rostrum; 2) Genu; 3,4,5) Rostral, anterior and posterior body, respectively; 6) Isthmus; 7) Splenium (see Fig. 2B). Following this schema, seven ROIs were delineated in the midsagittal plane. When necessary, spurious fibers were eliminated by adding excluding ROIs.

For all dissected tracts, the HMOA (hindrance modulated orientational anisotropy), an index employed as a surrogate for tract microstructural organization, was extracted. The mean HMOA is defined as the absolute amplitude of each lobe of the fiber orientation distribution; it is considered highly sensitive to axonal myelination, fiber diameter, and axonal density [61].

We performed six multiple linear regression analyses using the backward method, one per each dependent variable of interest (see Statistical behavioral analysis, indices section). In separate analyses, we used as predictors, either the mean HMOA of the right and left SLF I, II, and III, or the 7 portions of the CC.

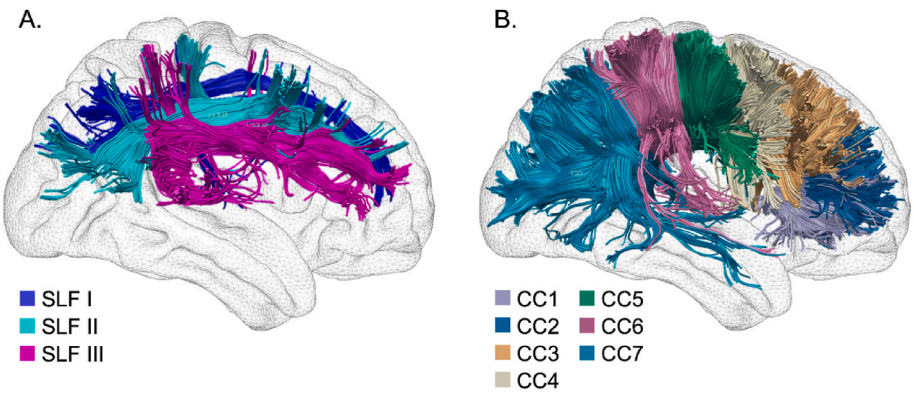

Fig. 2. Representation of an example dissection of **(A)** the three branches of the superior longitudinal fasciculus (SLF); SLF I, dorsal branch; SLF II, middle branch; SLF III, ventral branch. **(B)** The seven portions of the corpus callosum; CC1: Rostrum; CC2: Genu; CC3: rostral body; CC4: anterior body; CC5: posterior body; CC6: Isthmus; CC7: Splenium. For both panels, a sagittal view is presented, where the frontal cortex is on the right, and the occipital cortex is on the left.

2.6.2. Tract-Based Spatial Statistics (TBSS)

The diffusion tensor model was fitted using *dtifit* tool (FDT, FMRIB's Diffusion Toolbox), and common scalar maps (i.e., fractional anisotropy, FA) were subsequently computed. Then, it was brain-extracted using FSL's brain extraction tool BET [62]. The sequence of b-value = 1000 s/mm^2 was used for fitting the model; this was done because the tensor model is not good at fitting the signal for high b-values.

Voxelwise statistical analysis of the FA data was carried out using TBSS (Tract-Based Spatial Statistics [63], part of FSL [64]). First, all participants' FA data were aligned into a common space using the nonlinear registration tool FNIRT [65,66]. Next, the mean FA image was created and thinned to create a mean FA skeleton which represents the centers of all tracts common to the group. A threshold of FA>0.2 was selected to exclude voxels not belonging to white matter. Each participant's FA data was then projected onto this skeleton. Finally, the resulting map was fed into voxelwise nonparametric statistics using *randomise* [67]. The number of permutations was set to 5000 and multiple comparisons were corrected using the threshold-free cluster enhancement (TFCE) option. Six regression models were computed for the FA maps and one per each variable of interest (i.e., main effect of Region in reaction time (RT), accuracy, and proportion of seen targets, interaction between Attention and Region, and behavioral attentional effects; see Statistical behavioral analysis, indices section).

2.7. Statistical behavioral analysis

In our previous TMS studies, we used repeated-measured analysis of variance (ANOVAs) to analyze the behavioral data. Linear Mixed Models (LMM) have gained popularity as an alternative to repeated-measures ANOVAs in the field of experimental psychology [68], mainly because this framework offers various notable advantages over the traditional approach [69]. First, LMMs enable the explicit specification of random effects such as participant-level variations, rather than pooling this variability within an error term. Secondly, these models are more flexible when it comes to handling missing data as compared to ANOVAs, enhancing the robustness of the analysis. Finally, LMMs are also more robust to violations of distributional assumptions than traditional ANOVAs [70].

LMMs were conducted to analyze behavioral effects, using the pymer4 Python package [71] to calculate significance applying Satterthwaite's method to estimate degrees of freedom. In three different analyses, we included participants reaction times (RTs), accuracy, and the proportion of seen targets as the dependent variables, and the full fixed structure of the model contained the main effects of Region (FEF and Vertex), Task (orienting and alerting), Attention (attended or unattended) and Awareness (seen or unseen), as well as all possible interactions between them. The input provided to the models was the trial-level estimates for each participant. For RTs an inverse Gaussian distribution family was assumed, while for accuracy and proportion of seen targets the distribution was binomial. Note that the Awareness term is not introduced when the proportion of seen responses were analyzed. The random structure included the participant as an intercept and the trial as a random slope:

(Region + Task + Attention + Awareness + Region:Task + Region:Attention + Region:Awareness + Task:Attention + Task:Awareness + Attention:Awareness + Region:Task:Attention + Region:Task:Awareness + Region:Attention:Awareness + Task:Attention:Awareness + Region:Task:Attention:Awareness + (1+Trial|Participant))

Significance of fixed effects was assessed using F-tests and p-values from the model summary, and to qualify any interactions marginal estimates were computed and Bonferroni-corrected p-values were obtained for the post-hoc pairwise comparisons. Summary tables including the model estimates and the 95 % confidence interval for all analyses can be found in the Supplementary materials (Tables S4–S8).

The code for these analyses can be found here: https://github.com/rodriguez-p/WM_TMS.

2.7.1. Indices

Based on the behavioral results and to explore the relationship between TMS effects and white matter microstructural properties, we calculated the following indices:

From the main effect of Region in RT, accuracy, and the proportion of seen targets:

- RT (for seen targets) in left FEF minus vertex TMS.
- Accuracy (for seen targets) in vertex minus left FEF TMS.
- Proportion of seen targets in vertex minus left FEF TMS.

From the interaction between Region and Attention:

- RT (for seen targets) for unattended minus attended targets for left FEF minus vertex TMS.

Additionally, we created two indices of the behavioral attentional effect in the alerting and the orienting tasks, to explore whether RT attentional effects in each task could be explained by white matter microstructural properties [35]. We only considered vertex stimulation sessions to isolate the attentional effect from the TMS effect.

- RT (for seen targets) for no tone minus tone trials in the alerting task.
- RT (for seen targets) for invalid minus valid trials in the orienting task.

3. Results

3.1. Behavioral results

Table 1 summarizes the results of the three ANOVAs over RTs, accuracy, and the proportion of seen targets. Supplementary Tables 1–3 include the means and standard deviations for each variable and condition. A main effect of Region was observed on RTs, accuracy, and the proportion of seen targets. Mean RTs were slower when the left FEF was stimulated as compared to the vertex condition ($F(1, 20291.583) = 4.104$, $p = 0.043$, see Fig. 3, left panel), and this effect was larger for unseen than seen trials (interaction Region x Awareness ($F(1, 20295.748) = 25.210$, $p < 0.001$). Moreover, accuracy was impaired ($F(1, 22736.798) = 6.384$, $p = 0.011$) and the proportion of seen targets decreased ($F(1, 22743.020) = 12.459$, $p < 0.001$) when the left FEF was stimulated, as compared to the vertex condition (see Fig. 3, middle and right panels, respectively).

The main effect of Task was significant both in the RT and the proportion of seen target analysis. RTs were faster in the Orienting task as compared to the Alerting task ($t(20290.113) = 11.894$, $p_{Bonf} < 0.001$), and more targets were seen in the Orienting blocks as compared to the Alerting ones ($t(22742.212) = -9.135$, $p_{Bonf} < 0.001$). There was also a main effect of Attention both in the RT and the proportion of seen analyses. Responses were faster ($t(20290.220) = -13.693$, $p < 0.001$) and more targets were seen ($t(22742.448) = 14.680$, $p < 0.001$) in attended trials than in non-attended trials (i.e., tone present vs. absent trials in the alerting condition, and valid vs. invalid trials in the orienting condition). The main effect of Awareness was also significant, with faster ($F(1, 20306.567) = 134.299$, $p < 0.001$) and more accurate responses ($F(1, 22695.262) = 141.551$, $p < 0.001$) for seen than unseen trials. As several interactions in the RT analysis involved the term Awareness, we decided to follow up this analysis by conducting separate ANOVAs for seen and unseen trials (Table 2).

The previously described main effects of Region, Task, Attention, and the interaction between Task and Attention, were significant for both seen and unseen trials. For seen targets, there were also significant interactions between Region x Attention and Region x Task. The RT attentional effect increased when the left FEF was stimulated, as compared to the vertex condition [$F(1, 10612.454) = 6.389$, $p = 0.011$ (Fig. 4, top panel)]. Moreover, the main effect of Region on RTs was significant in the Alerting task, $t(10613.691) = -2.875$, $p_{Bonf} = 0.024$, and not in the Orienting task, $t(10613.978) = -0.319$, $p_{Bonf} > 0.05$ (Fig. 4, bottom panel).

3.2. Diffusion weighted imaging (DWI) analysis

3.2.1. DWI tractography

First, we explored whether the TMS effects could be predicted by individual differences in white matter microstructural properties of the SLF and CC. For the Region (i.e., TMS effect) over RT (i.e., slower RT for left FEF compared to vertex stimulation), the results of the regression analysis ($F(1,47) = 6.437$, $p = 0.015$, $R^2 = 0.120$) showed that the right SLF I was a significant predictor ($t = -2.537$, $p = 0.015$). That is, the higher the integrity of the right SLF I (reflected in the mean HMOA of the tract), the more reduced the TMS effect over RT (see Fig. 5A). In addition, results showed ($F(1,49) = 7.012$, $p = 0.011$, $R^2 = 0.127$) that the rostral body of the CC (section CC3) was a significant predictor of the Region effect over accuracy (reduced accuracy for left FEF compared to vertex stimulation; $t = 2.648$, $p = 0.011$). That is, the higher the integrity of this portion of the CC, the larger the TMS effect over accuracy (see Fig. 5A). No significant model was found for the Region effect over the proportion of seen targets (all ps > 0.062).

The index used for the observed interaction between Attention and Region (i.e., increased attentional effect when the left FEF was stimulated as compared to the vertex), was predicted by the integrity of the right SLF III ($t = -2.504$, $p = 0.016$; $F(1,48) = 6.270$, $p = 0.016$, $R^2 = 0.118$), and the posterior body of the CC (section CC5) ($t = -4.286$, $p < 0.001$; $F(1,49) = 18.369$, $p < 0.001$, $R^2 = 0.277$). That is, the lower the integrity of these tracts, the larger the interaction (see Fig. 5B).

Finally, we explored whether attentional effects (without considering TMS effects; i.e., in the vertex condition) could also be predicted by individual differences in white matter in each task. For the orienting task, results revealed that the right SLF III ($t = 2.655$, $p = 0.011$) was a significant predictor ($F(1, 48) = 7.050$, $p = 0.011$, $R^2 = 0.130$). The integrity of this tract was positively related with the orienting effect. That is, the higher the integrity of the right SLF III, the larger the attentional orienting effects over RT (see Fig. 5C). No significant model was found for the alerting task (all ps > 0.208).

3.2.2. TBSS analysis

This analysis revealed no correlation between the FA and the TMS effects in any of the behavioral indices (i.e., Region-TMS effects over RTs, accuracy, and the proportion of seen targets, and the interaction between Attention and Region). Additionally, to explore the possible role of inter-individual white matter variability in behavioral attentional effects (without considering the TMS effect), we performed regression analyses for the RT attentional effects for alerting and orienting tasks (i.e., slower RT for unattended as compared to attended trials). We found a significant negative correlation between the FA and the attentional

Table 1
Summary results for the ANOVA analyses on the variables RTs, accuracy, and the proportion of Seen stimuli, including the main effects of Region (FEF and Vertex), Task (orienting and alerting), Attention (attended or unattended), and Awareness (seen or unseen), and their interactions. Significant effects or interactions are highlighted in bold.

	Reaction times		Accuracy		Proportion Seen	
	F-stat	P-val	F-stat	P-val	F-stat	P-val
Awareness	**135.556**	**< .001**	**141.145**	**< .001**		
Attention	**189.025**	**< .001**	0.087	0.768	**215.945**	**< .001**
Region	**4.104**	**.043**	**6.397**	**.011**	**13.097**	**< .001**
Task	**141.734**	**< .001**	0.062	0.803	**102.200**	**< .001**
Awareness×Attention	0.055	0.815	0.200	0.654		
Awareness×Region	**24.946**	**< .001**	1.774	0.183		
Attention×Region	1.122	0.289	0.370	0.543	0.151	0.698
Awareness×Task	**5.772**	**.016**	1.911	0.167		
Attention×Task	**88.192**	**< .001**	0.921	0.337	0.001	0.974
Region×Task	2.155	0.142	0.360	0.548	0.010	0.919
Awareness×Attention×Region	**4.536**	**.033**	1.781	0.182		
Awareness×Attention×Task	**13.739**	**< .001**	0.098	0.755		
Awareness×Region×Task	0.634	0.426	1.001	0.317		
Attention×Region×Task	0.357	0.550	0.015	0.903	0.016	0.900
Awareness×Attention×Region×Task	0.543	0.461	1.015	0.314		

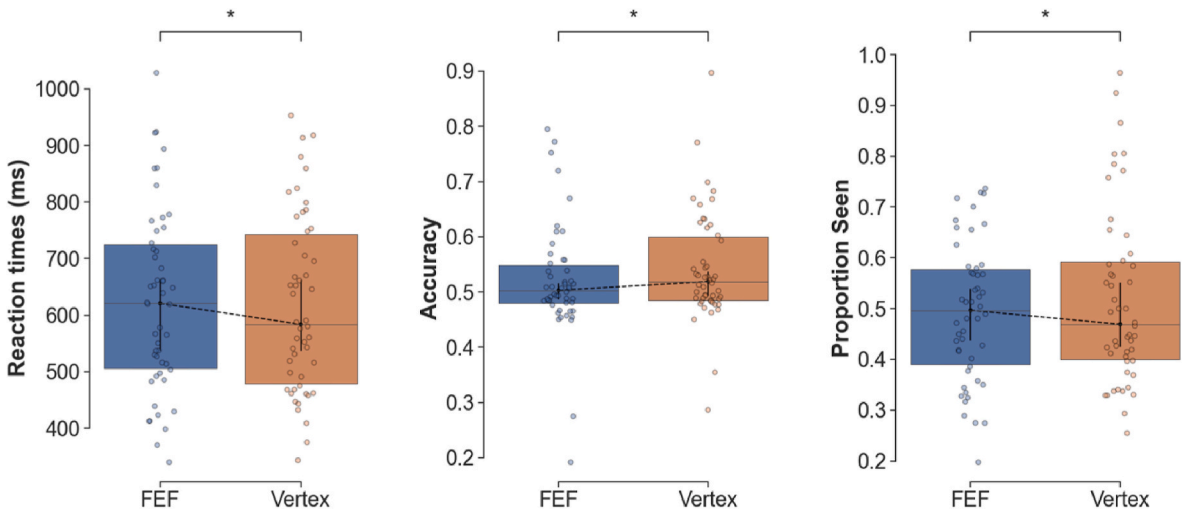

Fig. 3. Main effect of Region on RTs, accuracy, and proportion of seen targets. The maximum and minimum values per effect are represented in the whiskers of the box plots. The Interquartile range (IQR) is displayed in the boxes by portraying the lower quartile, median, and upper quartile. The colored dots represent mean values for each participant in each condition, and the dashed black line connects the median values of each condition. Asterisks indicate significant comparisons.

Table 2
Summary ANOVA table for the analyses over RTs separately for seen and unseen trials. Bold characters represent significant effects or interactions.

	Seen		Unseen	
	F-stat	P-val	F-stat	P-val
Attention	**120.339**	**< .001**	**83.780**	**< .001**
Region	**5.944**	**.015**	**21.740**	**< .001**
Task	**52.770**	**< .001**	**93.084**	**< .001**
Attention×Region	**6.174**	**.013**	0.390	0.532
Attention×Task	**18.987**	**< .001**	**83.507**	**< .001**
Region×Task	**3.949**	**.047**	0.256	0.613
Attention×Region×Task	1.303	0.254	0.010	0.920

effect in the alerting task (see Fig. 6). The analysis revealed two main clusters of results: an anterior cluster on the right hemisphere involving the inferior fronto-occipital fasciculus (IFOF), the anterior thalamic radiation, the forceps minor, and the genu and body of the CC, and a posterior cluster on the left hemisphere including the SLFs, the middle longitudinal fasciculus, the IFOF, the optic radiation, and the forceps major. The higher the FA in these regions, the more reduced the RT alerting effect. No significant results were found for the orienting task. Significant TBSS results maps can be found at https://neurovault.org/images/886864/.

4. Discussion

This study aimed to explore the role of white matter variability in TMS neuromodulatory effects by using a substantial sample of healthy participants (n = 50), which provides high statistical power and enhances replicability. We employed hypothesis-driven DWI tractography of the SLF and CC, along with additional whole-brain data-driven TBSS. Participants performed a perceptual task with near-threshold stimuli preceded by alerting and orienting attentional cues. cTBS was applied over the left FEF, an attentional region previously involved in attention and consciousness interactions during both alerting [31] and orienting [32], or an active TMS vertex condition.

Consistent with the expected inhibitory effect of cTBS, TMS over the left FEF slowed down RTs (especially in the alerting task), impaired accuracy in the objective task, and reduced the proportion of seen targets, as compared to the vertex condition. However, attentional effects increased, overall, when TMS was applied over the left FEF as compared to the vertex condition. These increased attentional effects after TMS

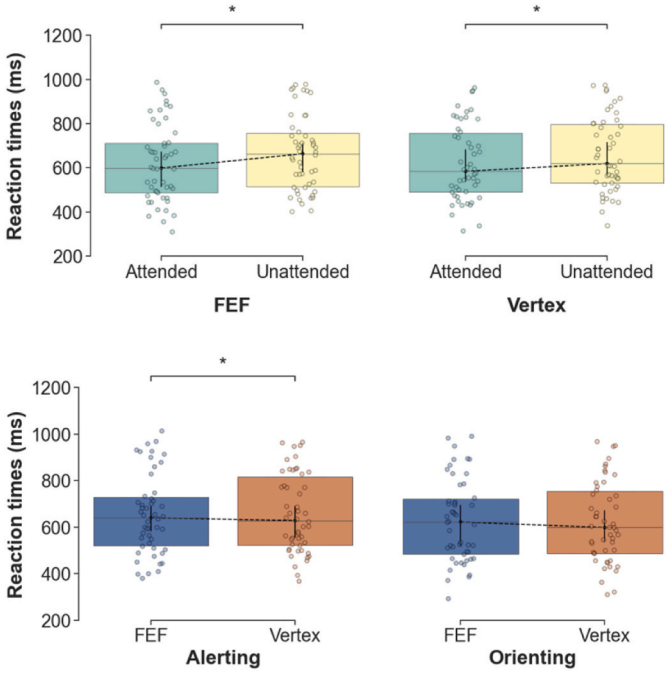

Fig. 4. Interactions between Region and Attention (top panel) and Region and Task (bottom panel) for trials reported as seen. The maximum and minimum values per effect are represented in the whiskers of the box plots. The Interquartile range (IQR) is displayed in the boxes by portraying the lower quartile, median, and upper quartile. The colored dots represent mean values for each participant in each condition, and the dashed black line connects the median values of each condition. Asterisks indicate significant comparisons.

have often been reported in literature [13,37]. In a similar vein, brain lesions affecting the parietal cortex [72] and the right IFOF have also been related to an increase in the use of alerting signals [73], which was associated with participants' capacity to accurately respond to unexpected (i.e., non-signaled) targets. All this evidence indicates that perturbation by TMS or lesions in attentional regions can sometimes lead to an increased use of attentional cues, which might be detrimental to respond to conditions in which the attentional cues are invalid or not present. As proposed by relevant attentional models [74], an optimal attentional system needs to be able to effectively pay attention while, at

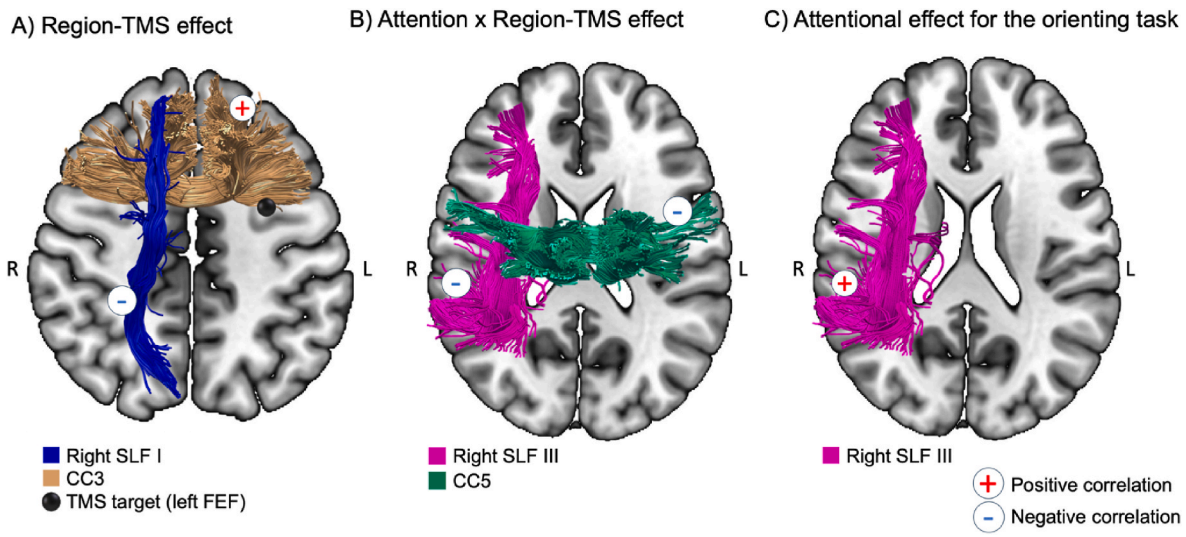

Fig. 5. Representation of the results of the multiple linear regression analyses for the DWI tractography and the behavioral effects. **(A)** Negative correlation between the right SLF I and the Region effect observed in the RT index; and positive correlation between the CC3 and the Region effect observed in the accuracy index. **(B)** Negative correlations between the right SLF III and the CC5 and the interaction between Attention (Attended vs. Unattended) and Region (left FEF vs. vertex) index. **(C)** Positive correlation between the RT behavioral attentional effect for the orienting task and the right SLF III.

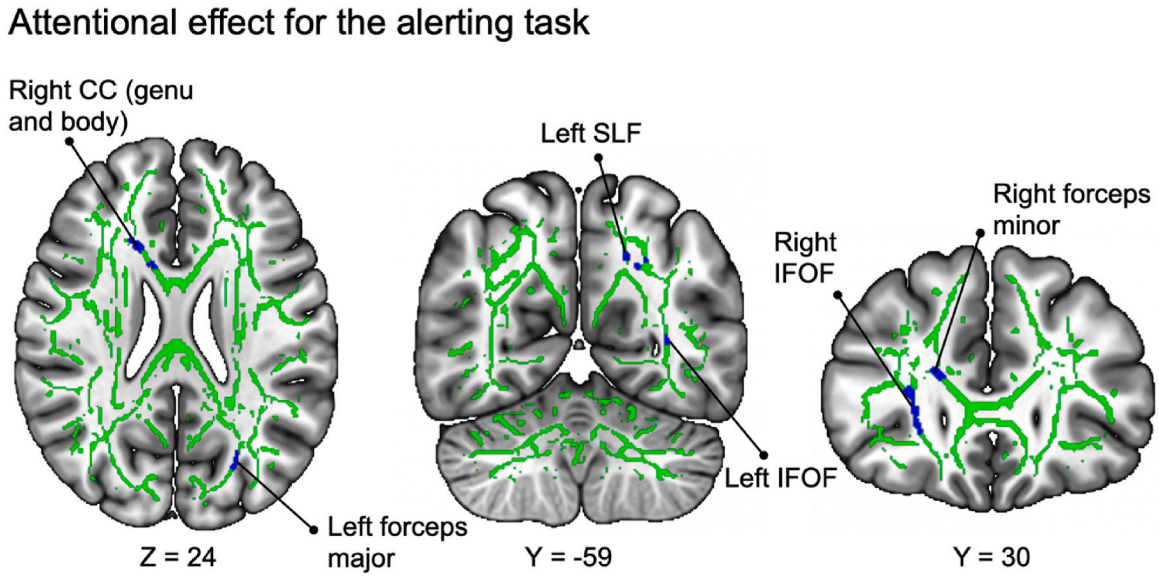

Fig. 6. Fractional anisotropy (FA) voxels identified with TBSS for the attentional effect over RT in the alerting task. Green voxels represent the white matter skeleton. Blue voxels represent significant results (TFCE corrected $p < 0.05$) with a negative correlation with behavior. (For interpretation of the references to color in this figure legend, the reader is referred to the Web version of this article.)

the same time, leaving some room for distraction and providing opportunities for attentional shifts to unexpected events.

White matter microstructural properties of tracts connecting fronto-parietal regions within the same hemisphere (i.e., the SLF) and the CC (which constitutes the main tract for interhemispheric connections) were related to the observed TMS effects. A negative correlation was observed between the TMS effect over RT and the integrity of the right SLF I. That is, an increased integrity of the right SLF I was associated with reduced TMS effects. In addition, attentional effects overall increased when TMS was applied to the left FEF as compared to the vertex condition. This increased attentional effect after TMS was also negatively related with the integrity of the right SLF III and the posterior body of the CC (portion CC5). This portion of the CC connects homologous posterior parietal areas, linking right and left attentional networks. These results critically replicate our previous observations [13–15], using different TMS protocols (cTBS in the present study, 1Hz repetitive TMS in Ref. [14], and online TMS pulses in Ref. [13,15]), and stimulating different brain regions (the left FEF in the present study, the supplementary motor area in Refs. [14,15], and the right superior parietal cortex in Ref. [13]).

This negative correlation between the microstructural properties of some white matter fasciculi and TMS effects has been interpreted as indicative of a compensatory mechanism. In particular, those participants with increased integrity in fronto-parietal pathways connecting key attentional regions, and portions of the CC that connect homologous attentional networks, are more resistant to the neuromodulatory effects of TMS over attentional functions. According to other proposals [16], when a brain network is affected by a short-term disruption in a particular node (such as that caused by TMS), alternative networks can be recruited to compensate for the affected cognitive function [17,75].

The functionality of this flexible network redistribution has been observed in several studies, where stimulating a single relevant network node did not produce a behavioral effect, but combined stimulation with a second node did (e.g., Ref. [76]). We propose that the structural connectivity would influence not only the propagation of TMS neural effects [3,11] but also the potential compensatory mechanisms that the system could employ. Participants with higher integrity in tracts connecting these relevant alternative networks (within or between them) may have an advantage in recruiting them, thereby compensating for the disrupted function and exhibiting less interference from TMS stimulation.

Similar results have been reported after brain damage. In the case of spatial neglect, lesions in the parietal cortex and its connections to the frontal lobe have been associated with attentional impairments and the severity of neglect [20]. This is in line with data showing that neglect patients have altered fronto(motor)-parietal connections in the contralesional hemisphere [77]. Moreover, lesions in the dorsolateral prefrontal cortex and the disconnection of the SLF III have been associated with perceptual impairments in contrast perception ([78], see also [79]). Altogether, this evidence suggests that white matter integrity of fronto-parietal and interhemispheric tracts is important in the healthy brain in situations of transient brain perturbation such as those induced by TMS, and in determining the presence and severity of attentional symptoms after brain damage.

As predicted based on previous studies (with brain damage [19,21], and healthy participants, [22]), there was a positive correlation between the TMS effect over accuracy and the rostral body of the CC (portion CC3), which connects homologous premotor and supplementary motor areas on each hemisphere [48], and thus also the left and right FEF [80,81] (see Fig. 5A). All our previous reports of white matter negative associations with TMS effects were related to fasciculi that did not innervate the stimulated region [13–15]. However, larger integrity of tracts directly connecting the stimulated region with homologous or other regions of the network could increase the TMS effects by the propagation of the signal. Indeed, experiments reveal that stimulation spreads to other regions of the brain, including deeper brain regions [4,5,82]. Several studies have previously proposed that the propagation of TMS pulses could occur through the structural connections between the stimulated region and other brain regions [3,6,83,84]. Concretely, TMS could trigger action potentials in the superficial neural tissue beneath the coil, which could then travel along neural pathways to reach connected cortical and subcortical structures [83]. Beynel et al. [5] also proposed that white matter tracts facilitate the co-activation of interconnected regions, modulating the functional connectivity between these regions. In addition, stimulation-induced interference in behavior is related to properties of white matter tracts [22,85].

White matter microstructural properties were also related to the observed attentional effects in the control condition (without considering the TMS effect; i.e., the vertex stimulation). This aligns with evidence indicating that variations in white matter characteristics underlying attentional networks are linked to individual differences in performance [86,87]. In the alerting task, the correlation was negative; that is, participants with lower integrity in several brain regions presented larger alerting effects. Attentional effects correlated negatively with the FA in the bilateral IFOF, right anterior thalamic radiation, left SLFs, left middle longitudinal fasciculus, left optic radiation, right forceps minor, and left forceps major, and the genu and body of the CC. Our results were consistent with previous observations by Luna et al. [35], who reported that participants with lower HMOA in the splenium of the CC presented an increased alerting effect. On the contrary, recent research [36] showed that the left anterior thalamic radiation, the left IFOF, and the left uncinate were associated with better use of the alerting signals. While the identified white matter tracts related with the alerting function were highly consistent with previous literature, more research is necessary to determine the specific role of the microstructural properties of those tracts in the effective use of alerting signals.

In the case of orienting, we observed a positive correlation between the integrity of the right SLF III and the orienting effect. That is, participants with increased integrity presented larger orienting effects. It is well established that the ventral network for attentional reorienting (which comprises the SLF III, [27]) is lateralized to the right hemisphere. Damage to this network, including SLF III disconnection, produces spatial neglect [41,88]. Our result consistently shows that, in healthy participants, increased integrity of this right hemisphere ventral branch of the SLF is associated with an increased use of orienting signals.

This study should be considered within the context of its limitations. Our hypothesis, which suggests that white matter integrity within alternative brain networks can compensate for TMS disruption, is supported by both the present findings and previous research. However, as brain functioning was not measured after TMS stimulation (for example, with fMRI), the proposed brain reorganization is inferred from the behavioral output. We propose future studies combining TMS, DWI, and fMRI methodologies to confirm and expand these results. In addition, as often found in TMS research [2], behavioral modulations caused by TMS exhibited high variability. Therefore, some participants showed a TMS effect in some of the behavioral variables while not in others. This factor makes it more difficult to predict those participants that will "respond" to the TMS stimulation from those that will "not respond", as it may depend on the specific measured output. We propose that complex data driven approaches, such as machine learning, could be used in future studies to reveal white matter complex patterns that could relate with such TMS variability. The proportion of variance explained by white matter properties can be considered medium (R^2 of around 0.12, [89]). This is coherent with the fact that many internal and external factors modulate TMS stimulation effects over behavior (see e.g., Ref. [2]). Among them, we explored white matter characteristics as one individual brain anatomical factor, but other brain factors such as morphological properties [90] or brain states could be considered [1]. This research contributes to understanding the variability in the neuromodulation of human behavior, acknowledging that it is not explained by a single factor but by a complex combination of factors. Finally, the main effect of Region reported in this study was also modest (as indicated by the estimates and the lower CIs approaching zero in some cases, see Supplementary Tables 4–8). This suggests that the Region effect is small and subjected to individual variability, as indicated by the correlation with the integrity of the SLF and the CC. This data is in line with Chechlacz et al. [22]. This study showed that when the TMS effects were more variable (left IPS as compared to right IPS stimulation), the contribution of the microstructural properties of the CC was higher. This may indicate that individual differences in white matter integrity contribute to explaining the variability in TMS effects, particularly when those effects are more inconsistent.

In conclusion, our study confirms the importance of the microstructural properties of white matter to explain part of the individual variability associated with TMS neuromodulation effects over behavior. Two qualitatively different results were observed: 1) negative correlations between association tracts not directly stimulated by the TMS protocol, and with the posterior body of the CC, which we interpret as a compensatory effect; and 2) positive correlations with the portion of the CC connecting the stimulated region with the opposite hemisphere, which we associate to the spread of TMS activation. Finally, we explored the relationship between white matter microstructural properties and behavioral attentional effects (not related to TMS), and observed interesting associations between alerting effects and the integrity of association, commissural, and projection fibers, as well as increased orienting effects in participants with high integrity of the right SLF III.

The results of this work open up new avenues for personalizing stimulation both in the laboratory and, hopefully, in future clinical practice. Behavioral outcomes following TMS application are diverse, often resulting in null or incongruent findings in TMS research [91,92], and inconsistent therapeutic outcomes [93]. Therefore, further investigation is needed to better understand individual variability in response

to neuromodulation. By gaining a comprehensive understanding of the sources of variability, including white matter properties, we could establish ways to control them or use them to enhance therapeutic efficacy.

CRediT authorship contribution statement

Mar Martín-Signes: Writing – review & editing, Writing – original draft, Investigation, Formal analysis. **Pablo Rodríguez-San Esteban:** Writing – review & editing, Writing – original draft, Investigation, Formal analysis. **Cristina Narganes-Pineda:** Writing – review & editing, Investigation. **Alfonso Caracuel:** Writing – review & editing, Investigation. **José Luís Mata:** Writing – review & editing, Investigation. **Elisa Martín-Arévalo:** Writing – review & editing, Writing – original draft, Investigation, Funding acquisition, Conceptualization. **Ana B. Chica:** Writing – review & editing, Writing – original draft, Investigation, Funding acquisition, Conceptualization.

Data availability

Behavioral data from the pilot and the experimental tasks, as well as the E-Prime files needed to run the task, are publicly available via Open Science Framework (https://osf.io/4jg3f/). DWI tractography measures and TBSS results maps can also be found at the OSF repository. Additionally, TBSS maps can be found in Neurovault for a convenient visualization (https://neurovault.org/images/886864/).

Code availability

Analyses were carried out using open software and toolboxes (see methods section). The Python code for the behavioral analyses can be found at the following repository: https://github.com/rodriguez-p/WM_TMS. DWI preprocessing routines and TBSS analysis were part of the FSL software tool, https://fsl.fmrib.ox.ac.uk/fsl/fslwiki/FEAT. Additionally, DWI tractography was performed with the softwares StarTrack (https://www.mr-startrack.com/) and TrackVis (https://trackvis.org/). Linear regression analyses were performed with JASP (https://jasp-stats.org/).

Funding

This research was supported by grant PID2020-119033GB-I00 funded by MICIU/AEI/10.13039/501100011033 to A.B.C. and by FEDER/Junta de Andalucía-Consejería de Economía y Conocimiento/project A. SEJ.090. UGR18 (awarded to A.B.C. and E.M.A.). E.M.A. is supported by the research project PID2020-116342 GA-I00, funded by MCIN/AEI/10.13039/501100011033. M.M.S. is supported by a postdoctoral contract for Young Researchers (PAIDI 2020) by the Ministry of Economy, Knowledge, Enterprise, and Universities of Andalusia.

Declaration of competing interest

The authors declare that they have no known competing financial interests or personal relationships that could have appeared to influence the work reported in this paper.

Appendix A. Supplementary data

Supplementary data to this article can be found online at https://doi.org/10.1016/j.brs.2024.11.006.

References

[1] Gießing C, Alavash M, Herrmann CS, Hilgetag CC, Thiel CM. Individual differences in local functional brain connectivity affect TMS effects on behavior. Sci Rep 2020;10(1):1–12. https://doi.org/10.1038/s41598-020-67162-8. 2020 10:1.

[2] Hartwigsen G, Silvanto J. Noninvasive brain stimulation: multiple effects on cognition. Neuroscientist : A Rev J Bringing Neurobiol, Neurol Psychiatr 2023;29(5):639–53. https://doi.org/10.1177/10738584221113806.

[3] Momi D, Ozdemir RA, Tadayon E, Boucher P, Di Domenico A, Fasolo M, Shafi MM, Pascual-Leone A, Santarnecchi E, Marcus A. Perturbation of resting-state network nodes preferentially propagates to structurally rather than functionally connected regions. Sci Rep 2021;11:12458. https://doi.org/10.1038/s41598-021-90663-z.

[4] Ruff CC, Driver J, Bestmann S. Combining TMS and fMRI: from 'virtual lesions' to functional-network accounts of cognition. Cortex 2009;45(9):1043–9. https://doi.org/10.1016/J.CORTEX.2008.10.012.

[5] Beynel L, Powers JP, Appelbaum LG. Effects of repetitive transcranial magnetic stimulation on resting-state connectivity: a systematic review. Neuroimage 2020;116596. https://doi.org/10.1016/j.neuroimage.2020.116596.

[6] Vink JJT, Mandija S, Petrov PI, van den Berg CAT, Sommer IEC, Neggers SFW. A novel concurrent TMS-fMRI method to reveal propagation patterns of prefrontal magnetic brain stimulation. Hum Brain Mapp 2018;39(11):4580–92. https://doi.org/10.1002/HBM.24307.

[7] Bergmann TO, Varatheeswaran R, Hanlon CA, Madsen KH, Thielscher A, Siebner HR. Concurrent TMS-fMRI for causal network perturbation and proof of target engagement. Neuroimage 2021;237:118093. https://doi.org/10.1016/J.NEUROIMAGE.2021.118093.

[8] Nummenmaa A, McNab JA, Savadjiev P, Okada Y, Hämäläinen MS, Wang R, Wald LL, Pascual-Leone A, Wedeen VJ, Raij T. Targeting of white matter tracts with transcranial magnetic stimulation. Brain Stimul 2014;7(1):80–4. https://doi.org/10.1016/J.BRS.2013.10.001.

[9] O'Shea J, Taylor PCJ, Rushworth MFS. Imaging causal interactions during sensorimotor processing. Cortex; a J Devoted Stud Nerv Syst Behav 2008;44(5):598–608. https://doi.org/10.1016/J.CORTEX.2007.08.012.

[10] McCann H, Pisano G, Beltrachini L. Variation in reported human head tissue electrical conductivity values. Brain Topogr 2019;32(5):825–58. https://doi.org/10.1007/S10548-019-00710-2.

[11] Momi D, Ozdemir RA, Tadayon E, Boucher P, Shafi MM, Pascual-Leone A, Santarnecchi E. Network-level macroscale structural connectivity predicts propagation of transcranial magnetic stimulation. Neuroimage 2021;229:117698. https://doi.org/10.1016/J.NEUROIMAGE.2020.117698.

[12] Stam CJ, van Straaten ECW, Van Dellen E, Tewarie P, Gong G, Hillebrand A, Meier J, Van Mieghem P. The relation between structural and functional connectivity patterns in complex brain networks. Int J Psychophysiol 2016;103:149–60. https://doi.org/10.1016/J.IJPSYCHO.2015.02.011.

[13] Botta F, Lupiáñez J, Santangelo V, Martín-Arévalo E. Transcranial magnetic stimulation of the right superior parietal lobule modulates the retro-cue benefit in visual short-term memory. Brain Sci 2021;11(2):1–15. https://doi.org/10.3390/BRAINSCI11020252.

[14] Martín-Signes M, Pérez-Serrano C, Chica AB. Causal contributions of the SMA to alertness and consciousness interactions. Cerebr Cortex 2019;29(2):648–56. https://doi.org/10.1093/cercor/bhx346.

[15] Martín-Signes M, Cano-Melle C, Chica AB. Fronto-parietal networks underlie the interaction between executive control and conscious perception: evidence from TMS and DWI. Cortex 2021;134:1–15. https://doi.org/10.1016/j.cortex.2020.09.027.

[16] Hartwigsen G. Flexible redistribution in cognitive networks. Trends Cognit Sci 2018;22(8):687–98. https://doi.org/10.1016/j.tics.2018.05.008. Elsevier Ltd.

[17] Turker S, Kuhnke P, Schmid FR, Cheung VKM, Weise K, Knoke M, Zeidler B, Seidel K, Eckert L, Hartwigsen G. Adaptive short-term plasticity in the typical reading network. Neuroimage 2023;281:120373. https://doi.org/10.1016/j.neuroimage.2023.120373.

[18] Bozzali M, Mastropasqua C, Cercignani M, Giulietti G, Bonnì S, Caltagirone C, Koch G. Microstructural damage of the posterior corpus callosum contributes to the clinical severity of neglect. PLoS One 2012;7(10). https://doi.org/10.1371/JOURNAL.PONE.0048079.

[19] Lunven M, De Schotten MT, Bourlon C, Duret C, Migliaccio R, Rode G, Bartolomeo P. White matter lesional predictors of chronic visual neglect: a longitudinal study. Brain 2015;138(3):746–60. https://doi.org/10.1093/brain/awu389.

[20] Lunven M, Rode G, Bourlon C, Duret C, Migliaccio R, Chevrillon E, Thiebaut de Schotten M, Bartolomeo P. Anatomical predictors of successful prism adaptation in chronic visual neglect. Cortex 2019;120:629–41. https://doi.org/10.1016/j.cortex.2018.12.004.

[21] Nyffeler T, Vanbellingen T, Kaufmann BC, Pflugshaupt T, Bauer D, Frey J, Chechlacz M, Bohlhalter S, Müri RM, Nef T, Cazzoli D. Theta burst stimulation in neglect after stroke: functional outcome and response variability origins. Brain 2019;142(4):992–1008. https://doi.org/10.1093/brain/awz029.

[22] Chechlacz M, Humphreys GW, Sotiropoulos SN, Kennard C, Cazzoli D. Structural organization of the corpus callosum predicts attentional shifts after continuous theta burst stimulation. J Neurosci 2015;35(46):15353–68. https://doi.org/10.1523/JNEUROSCI.2610-15.2015.

[23] Bloom JS, Hynd GW. The role of the corpus callosum in interhemispheric transfer of information: excitation or inhibition? Neuropsychol Rev 2005;15(2):59–71. https://doi.org/10.1007/S11065-005-6252-Y/METRICS.

[24] Kinsbourne M. Hemi-neglect and hemisphere rivalry. In: Weinstein EA, Friedland RP, editors. Hemi- inattention and hemisphere specialization. Raven; 1977. p. 41–9.

[25] Niogi S, Mukherjee P, Ghajar J, McCandliss BD. Individual differences in distinct components of attention are linked to anatomical variations in distinct white matter tracts. Front Neuroanat 2010;4:1–12. https://doi.org/10.3389/neuro.05.002.2010.

[26] Corbetta M, Patel G, Shulman GL. The reorientingto system of the human brain: from environment to theory of Mind. Neuron 2008;58(3):306–24.
[27] Thiebaut de Schotten M, Dell'Acqua F, Forkel SJ, Simmons A, Vergani F, Murphy DGM, Catani M. A lateralized brain network for visuospatial attention. Nat Neurosci 2011;14(10):1245–7. https://doi.org/10.1038/nn.2905.
[28] Coull JT, Nobre AC, Frith CD. The noradrenergic α2 agonist clonidine modulates behavioural and neuroanatomical correlates of human attentional orienting and alerting. Cerebr Cortex 2001;11(1):73–84. https://doi.org/10.1093/cercor/11.1.73.
[29] Fan J, McCandliss BD, Fossella J, Flombaum JI, Posner MI. The activation of attentional networks. Neuroimage 2005;26(2):471–9. https://doi.org/10.1016/j.neuroimage.2005.02.004.
[30] Yanaka HT, Saito DN, Uchiyama Y, Sadato N. Neural substrates of phasic alertness: a functional magnetic resonance imaging study. Neurosci Res 2010;68(1):51–8. https://doi.org/10.1016/j.neures.2010.05.005.
[31] Chica AB, Bayle DJ, Botta F, Bartolomeo P, Paz-Alonso PM. Interactions between phasic alerting and consciousness in the fronto-striatal network. Sci Rep 2016;6:31868. https://doi.org/10.1038/srep31868.
[32] Chica AB, Paz-Alonso PM, Valero-Cabre A, Bartolomeo P. Neural bases of the interactions between spatial attention and conscious perception. Cerebr Cortex 2013;23(6):1269–79. https://doi.org/10.1093/cercor/bhs087.
[33] Hunt E, Pellegrino JW, Yee PL. Individual differences in attention. Psychol of Learn Motiv - Adv Res Theor of Learning and Motivation - Advances in Research and Theory 1989;24(C):285–310. https://doi.org/10.1016/S0079-7421(08)60540-X.
[34] Ge H, Yin X, Xu J, Tang Y, Han Y, Xu W, Pang Z, Meng H, Liu S. Fiber pathways of attention subnetworks revealed with tract-based spatial statistics (TBSS) and probabilistic tractography. PLoS One 2013;8(11):1–7. https://doi.org/10.1371/journal.pone.0078831.
[35] Luna FG, Lupiáñez J, Martín-Arévalo E. Microstructural white matter connectivity underlying the attentional networks system. Behav Brain Res 2021;401:113079. https://doi.org/10.1016/j.bbr.2020.113079.
[36] Martín-Signes M, Paz-Alonso PM, Thiebaut de Schotten M, Chica AB. Integrating brain function and structure in the study of the human attentional networks: a functionnectome study. Brain Struct Funct 2024. https://doi.org/10.1007/S00429-024-02824-1.
[37] Martín-Arévalo E, Lupiáñez J, Narganes-Pineda C, Marino G, Colás I, Chica AB. The causal role of the left parietal lobe in facilitation and inhibition of return. Cortex 2019;117:311–22. https://doi.org/10.1016/J.CORTEX.2019.04.025.
[38] Chica AB, Valero-Cabré A, Paz-Alonso PM, Bartolomeo P. Causal contributions of the left frontal eye field to conscious perception. Cerebr Cortex 2014;24(3):745–53. https://doi.org/10.1093/cercor/bhs357.
[39] Grosbras MH, Paus T. Transcranial magnetic stimulation of the human frontal eye field: effects on visual perception and attention. J Cognit Neurosci 2002;14(7):1109–20. https://doi.org/10.1162/089892902320474553.
[40] Muggleton NG, Juan C-H, Cowey A, Walsh V. Human frontal eye fields and visual search. J Neurophysiol 2003;89(6):3340–3. https://doi.org/10.1152/jn.01086.2002.
[41] Bartolomeo P, Thiebaut de Schotten M, Doricchi F. Left unilateral neglect as a disconnection syndrome. Cerebr Cortex 2007;17(11):2479–90. https://doi.org/10.1093/cercor/bhl181.
[42] Ciaraffa F, Castelli G, Parati EA, Bartolomeo P, Bizzi A. Visual neglect as a disconnection syndrome? A confirmatory case report. Neurocase 2013;19(4):351–9. https://doi.org/10.1080/13554794.2012.667130.
[43] Doricchi F, Thiebaut de Schotten M, Tomaiuolo F, Bartolomeo P. White matter (dis)connections and gray matter (dys)functions in visual neglect: gaining insights into the brain networks of spatial awareness. Cortex 2008;44(8):983–95. https://doi.org/10.1016/j.cortex.2008.03.006.
[44] Lunven M, Bartolomeo P. Attention and spatial cognition: neural and anatomical substrates of visual neglect. Ann Phys Rehabil Med 2017;60:124–9. https://doi.org/10.1016/j.rehab.2016.01.004.
[45] Carretié L, Ríos M, Periáñez JA, Kessel D, Álvarez-Linera J. The role of low and high spatial frequencies in exogenous attention to biologically salient stimuli. PLoS One 2012;7(5):1–8. https://doi.org/10.1371/journal.pone.0037082.
[46] Faul F, Erdfelder E, Lang AG, Buchner A. G*Power 3: a flexible statistical power analysis program for the social, behavioral, and biomedical sciences. Behav Res Methods 2007;39(2):175–91. https://link.springer.com/content/pdf/10.3758/BF03193146.pdf.
[47] Rojkova K, Volle E, Urbanski M, Humbert F, Dell'Acqua F, Thiebaut de Schotten M. Atlasing the frontal lobe connections and their variability due to age and education: a spherical deconvolution tractography study. Brain Struct Funct 2016;221(3):1751–66. https://doi.org/10.1007/s00429-015-1001-3.
[48] Witelson SF. Hand and sex differences in the isthmus and genu of the human corpus callosum. A postmortem morphological study. Brain : J Neurol 1989;112(3):799–835. https://doi.org/10.1093/BRAIN/112.3.799. Pt 3.
[49] Rossi S, Antal A, Bestmann S, Bikson M, Brewer C, Brockmöller J, Carpenter LL, Cincotta M, Chen R, Daskalakis JD, Di Lazzaro V, Fox MD, George MS, Gilbert D, Kimiskidis VK, Koch G, Ilmoniemi RJ, Pascal Lefaucheur J, Leocani L, Hallett M. Safety and recommendations for TMS use in healthy subjects and patient populations, with updates on training, ethical and regulatory issues: expert Guidelines. Clin Neurophysiol 2021;132(1):269–306. https://doi.org/10.1016/J.CLINPH.2020.10.003.
[50] Schneider W, Eschman A, Zuccolotto A, Burgess S, Cernicky B, Gilkey D, Gliptis J, Maciejczyk V, Macwhinney B, Rodgers K, James JS. E-Prime user's guide. Psychol Software Tools, Inc; 2002.
[51] Caulfield KA, Fleischmann HH, Cox CE, Wolf JP, George MS, McTeague LM. Neuronavigation maximizes accuracy and precision in TMS positioning: evidence from 11,230 distance, angle, and electric field modeling measurements. Brain Stimul 2022;15(5):1192–205. https://doi.org/10.1016/J.BRS.2022.08.013.
[52] Huang YZ, Edwards MJ, Rounis E, Bhatia KP, Rothwell JC. Theta burst stimulation of the human motor cortex. Neuron 2005;45(2):201–6. https://doi.org/10.1016/j.neuron.2004.12.033.
[53] Nyffeler T, Wurtz P, Lüscher H-R, Hess CW, Senn W, Pflugshaupt T, Von Wartburg R, Lüthi M, Müri RM. Repetitive TMS over the human oculomotor cortex: comparison of 1-Hz and theta burst stimulation. Neurosci Lett 2006;409:57–60. https://doi.org/10.1016/j.neulet.2006.09.011.
[54] Rossini PM, Burke D, Chen R, Cohen LG, Daskalakis Z, Di Iorio R, Di Lazzaro V, Ferreri F, Fitzgerald PB, George MS, Hallett M, Lefaucheur JP, Langguth B, Matsumoto H, Miniussi C, Nitsche MA, Pascual-Leone A, Paulus W, Rossi S, Ziemann U. Non-invasive electrical and magnetic stimulation of the brain, spinal cord, roots and peripheral nerves: basic principles and procedures for routine clinical and research application. An updated report from an I.F.C.N. Committee. Clin Neurophysiol : Off J Int Fed Clin Neurophysiol 2015;126(6):1071–107. https://doi.org/10.1016/J.CLINPH.2015.02.001.
[55] Jung J, Bungert A, Bowtell R, Jackson SR. Vertex stimulation as a control site for transcranial magnetic stimulation: a concurrent TMS/fMRI study. Brain Stimul 2016;9(1):58–64. https://doi.org/10.1016/j.brs.2015.09.008.
[56] Andersson JLR, Skare S, Ashburner J. How to correct susceptibility distortions in spin-echo echo-planar images: application to diffusion tensor imaging. Neuroimage 2003;20(2):870–88. https://doi.org/10.1016/S1053-8119(03)00336-7.
[57] Andersson JLR, Sotiropoulos SN. An integrated approach to correction for off-resonance effects and subject movement in diffusion MR imaging. Neuroimage 2016;125:1063–78. https://doi.org/10.1016/J.NEUROIMAGE.2015.10.019.
[58] Bastiani M, Cottaar M, Fitzgibbon SP, Suri S, Alfaro-Almagro F, Sotiropoulos SN, Jbabdi S, Andersson JLR. Automated quality control for within and between studies diffusion MRI data using a non-parametric framework for movement and distortion correction. Neuroimage 2019;184:801–12. https://doi.org/10.1016/J.NEUROIMAGE.2018.09.073.
[59] Guo F, Leemans A, Viergever MA, Dell'Acqua F, De Luca A. Generalized Richardson-Lucy (GRL) for analyzing multi-shell diffusion MRI data. Neuroimage 2020;218:116948. https://doi.org/10.1016/J.NEUROIMAGE.2020.116948.
[60] Wang R, Benner T, Sorensen AG, Wedeen VJ. Diffusion toolkit : a software package for diffusion imaging data processing and tractography. Proc Int Soc Magn Reson Med 2007;15:3720. https://doi.org/10.1128/MCB.25.11.4371.
[61] Dell'Acqua, Simmons A, Williams SCR, Catani M. Can spherical deconvolution provide more information than fiber orientations? Hindrance modulated orientational anisotropy, a true-tract specific index to characterize white matter diffusion. Hum Brain Mapp 2013;34(10):2464–83. https://doi.org/10.1002/hbm.22080.
[62] Smith SM. Fast robust automated brain extraction. Hum Brain Mapp 2002;17(3):143–55. https://doi.org/10.1002/hbm.10062.
[63] Smith SM, Jenkinson M, Johansen-Berg H, Rueckert D, Nichols TE, Mackay CE, Watkins KE, Ciccarelli O, Cader MZ, Matthews PM, Behrens TEJ. Tract-based spatial statistics: voxelwise analysis of multi-subject diffusion data. Neuroimage 2006;31(4):1487–505. https://doi.org/10.1016/j.neuroimage.2006.02.024.
[64] Smith SM, Jenkinson M, Woolrich MW, Beckmann CF, Behrens TEJ, Johansen-Berg H, Bannister PR, De Luca M, Drobnjak I, Flitney DE, Niazy RK, Saunders J, Vickers J, Zhang Y, De Stefano N, Brady JM, Matthews PM. Advances in functional and structural MR image analysis and implementation as FSL. Neuroimage 2004;23(SUPPL. 1):S208–19. https://doi.org/10.1016/J.NEUROIMAGE.2004.07.051.
[65] Andersson JLR, Jenkinson M, Smith S. Non-linear registration aka spatial normalisation FMRIB technial report TR07JA2. www.fmrib.ox.ac.uk/analysis/techrep; 2007.
[66] Andersson JLR, Jenkinson M, Smith S. Non-linear optimisation FMRIB technial report TR07JA1. www.fmrib.ox.ac.uk/analysis/techrep; 2007.
[67] Winkler AM, Ridgway GR, Webster MA, Smith SM, Nichols TE. Permutation inference for the general linear model. Neuroimage 2014;92:381–97. https://doi.org/10.1016/J.NEUROIMAGE.2014.01.060.
[68] Magezi DA. Linear mixed-effects models for within-participant psychology experiments: an introductory tutorial and free, graphical user interface (LMMgui). Front Psychol 2015;6(JAN):110312. https://doi.org/10.3389/FPSYG.2015.00002/BIBTEX.
[69] Lo S, Andrews S. To transform or not to transform: using generalized linear mixed models to analyse reaction time data. Front Psychol 2015;6. https://doi.org/10.3389/FPSYG.2015.01171.
[70] Schielzeth H, Dingemanse NJ, Nakagawa S, Westneat DF, Allegue H, Teplitsky C, Réale D, Dochtermann NA, Garamszegi LZ, Araya-Ajoy YG. Robustness of linear mixed-effects models to violations of distributional assumptions. Methods Ecol Evol 2020;11(9):1141–52. https://doi.org/10.1111/2041-210X.13434.
[71] Jolly E. Pymer4: connecting R and Python for linear mixed modeling. J Open Source Softw 2018;3(31):862. https://doi.org/10.21105/JOSS.00862.
[72] Chica AB, Thiebaut de Schotten M, Toba M, Malhotra P, Lupiáñez J, Bartolomeo P. Attention networks and their interactions after right-hemisphere damage. Cortex; a J Devoted Stud Nerv Syst Behav 2012;48(6):654–63. https://doi.org/10.1016/J.CORTEX.2011.01.009.
[73] Colás-Blanco I, Chica AB, Thiebaut de Schotten M, Busquier H, Olivares G, Triviño M. Impaired attention mechanisms in confabulating patients: a VLSM and DWI study. Cortex 2023;159:175–92. https://doi.org/10.1016/J.CORTEX.2022.09.017.
[74] Fiebelkorn IC, Kastner S. Functional specialization in the attention network. Annu Rev Psychol 2020;71(1):221–49. https://doi.org/10.1146/annurev-psych-010418-103429.

[75] Martin S, Frieling R, Saur D, Hartwigsen G. TMS over the pre-SMA enhances semantic cognition via remote network effects on task-based activity and connectivity. Brain Stimul 2023;16(5):1346–57. https://doi.org/10.1016/j.brs.2023.09.009.
[76] Gallotto S, Schuhmann T, Duecker F, Middag-van Spanje M, de Graaf TA, Sack AT. Concurrent frontal and parietal network TMS for modulating attention. iScience 2022;25(3):103962. https://doi.org/10.1016/J.ISCI.2022.103962.
[77] Koch G, Oliveri M, Cheeran B, Ruge D, Gerfo E Lo, Salerno S, Torriero S, Marconi B, Mori F, Driver J, Rothwell JC, Caltagirone C. Hyperexcitability of parietal-motor functional connections for the intact left-hemisphere in neglect patients. Brain : J Neurol 2008;131(Pt 12):3147. https://doi.org/10.1093/BRAIN/AWN273.
[78] Colás I, Chica AB, Ródenas E, Busquier H, Olivares G, Triviño M. Conscious perception in patients with prefrontal damage. Neuropsychologia 2019;129:284–93. https://doi.org/10.1016/j.neuropsychologia.2019.03.002.
[79] Reuter F, Del Cul A, Malikova I, Naccache L, Confort-Gouny S, Cohen L, Cherif AA, Cozzone PJ, Pelletier J, Ranjeva JP, Dehaene S, Audoin B. White matter damage impairs access to consciousness in multiple sclerosis. Neuroimage 2009;44(2):590–9. https://doi.org/10.1016/j.neuroimage.2008.08.024.
[80] Tehovnik EJ, Sommer MA, Chou IH, Slocum WM, Schiller PH. Eye fields in the frontal lobes of primates. Brain Res Rev 2000;32(2–3):413–48. https://doi.org/10.1016/S0165-0173(99)00092-2.
[81] Vernet M, Quentin R, Chanes L, Mitsumasu A, Valero-Cabre A. Frontal eye field, where art thou? Anatomy, function, and non-invasive manipulation of frontal regions involved in eye movements and associated cognitive operations. Front Integr Neurosci 2014;8:1–24. https://doi.org/10.3389/fnint.2014.00066.
[82] Bestmann S, Baudewig J, Siebner HR, Rothwell JC, Frahm J. Functional MRI of the immediate impact of transcranial magnetic stimulation on cortical and subcortical motor circuits. Eur J Neurosci 2004;19(7):1950–62. https://doi.org/10.1111/J.1460-9568.2004.03277.X.
[83] Geeter N De, Dupré L, Crevecoeur G. Modeling transcranial magnetic stimulation from the induced electric fields to the membrane potentials along tractography-based white matter fiber tracts. J Neural Eng 2016;13(2):026028. https://doi.org/10.1088/1741-2560/13/2/026028.
[84] Siebner HR, Funke K, Aberra AS, Antal A, Bestmann S, Chen R, Classen J, Davare M, Di Lazzaro V, Fox PT, Hallett M, Karabanov AN, Kesselheim J, Beck MM, Koch G, Liebetanz D, Meunier S, Miniussi C, Paulus W, Ugawa Y. Transcranial magnetic stimulation of the brain: what is stimulated? - a consensus and critical position paper. Clin Neurophysiol : Off J Int Fed Clin Neurophysiol 2022;140:59–97. https://doi.org/10.1016/J.CLINPH.2022.04.022.
[85] Quentin R, Chanes L, Migliaccio R, Valabrègue R, Valero-Cabré A. Fronto-tectal white matter connectivity mediates facilitatory effects of non-invasive neurostimulation on visual detection. Neuroimage 2013;82:344–54. https://doi.org/10.1016/j.neuroimage.2013.05.083.
[86] Tuch DS, Salat DH, Wisco JJ, Zaleta AK, Hevelone ND, Rosas HD. Choice reaction time performance correlates with diffusion anisotropy in white matter pathways supporting visuospatial attention. Proc Natl Acad Sci USA 2005;102(34):12212–7. https://doi.org/10.1073/PNAS.0407259102/ASSET/AAEAEFE3-5F7C-42AB-8422-2729F82C7E42/ASSETS/GRAPHIC/ZPQ0340592580005.JPEG.
[87] Walhovd KB, Fjell AM. White matter volume predicts reaction time instability. Neuropsychologia 2007;45(10):2277–84. https://doi.org/10.1016/J.NEUROPSYCHOLOGIA.2007.02.022.
[88] Toba MN, Migliaccio R, Potet A, Pradat-Diehl P, Bartolomeo P. Right-side spatial neglect and white matter disconnection after left-hemisphere strokes. Brain Struct Funct 2022;227(9):2991–3000. https://doi.org/10.1007/S00429-022-02541-7.
[89] Miles J. R squared, adjusted R squared. Wiley StatsRef: Statistics Reference Online; 2014. https://doi.org/10.1002/9781118445112.STAT06627.
[90] Aberra AS, Wang B, Grill WM, Peterchev AV. Simulation of transcranial magnetic stimulation in head model with morphologically-realistic cortical neurons. Brain Stimul 2020;13(1):175–89. https://doi.org/10.1016/J.BRS.2019.10.002.
[91] De Graaf TA, Sack AT. Null results in TMS: from absence of evidence to evidence of absence. Neurosci Biobehav Rev 2011;35(3):871–7. https://doi.org/10.1016/J.NEUBIOREV.2010.10.006.
[92] Magnuson J, Ozdemir MA, Mathieson E, Kirkman S, Passera B, Rampersad S, Dufour AB, Brooks D, Pascual-Leone A, Fried PJ, Shafi MM, Ozdemir RA. Neuromodulatory effects and reproducibility of the most widely used repetitive transcranial magnetic stimulation protocols. PLoS One 2023;18(6):e0286465. https://doi.org/10.1371/JOURNAL.PONE.0286465.
[93] Terranova C, Rizzo V, Cacciola A, Chillemi G, Calamuneri A, Milardi D, Quartarone A. Is there a future for non-invasive brain stimulation as a therapeutic tool? Front Neurol 2019;10(JAN):398466. https://doi.org/10.3389/FNEUR.2018.01146/BIBTEX.